TRANSPORT PROBLEMS 2019 Volume 14 Issue 2
PROBLEMY TRANSPORTU DOI: 10.20858/tp.2019.14.2.1

Keywords: vehicle safety; hydro mechanical energy absorber; absorption of kinetic energy; mathematical model; dynamics process

Marijonas BOGDEVIČIUS*
Vilnius Gediminas Technical University
Sauletekio Ave. 11, LT 10223 Vilnius, Lithuania
Rolandas VITKŪNAS
Vilnius College of Technologies and Design
Antakalnio St. 54, LT-10303 Vilnius, Lithuania
**Corresponding author*. E-mail: marijonas.bogdevicius@vgtu.lt

HYDRO PNEUMATIC MECHANICAL ENERGY ABSORBER ENHANCING PASSIVE SAFETY OF A MOTOR VEHICLE

Summary. The purpose of this paper is to describe and analyse a mechanical device designed to enhance the safety of a motor vehicle. The topic is addressed by analysing the method of absorbing kinetic energy during a car collision with an obstacle. The article analyses opportunities to convert motor vehicle's kinetic energy into another type of energy in the case of collision. For this purpose, various mechanical, hydraulic or pneumatic devices are normally used. Such devices are designed to absorb collision energy and reduce or eliminate its impact on the driver, the passengers or cargo in the motor vehicle. The absorber may be used as an additional element of safety to the passenger and the cargo. The energy absorber described in the present article incorporates hydraulic, pneumatic and mechanical components. The description of the absorber presented here is based on mathematical calculations characterizing mechanical, pneumatic and hydraulic processes in the equipment. The analysis of the developed mechanism employs a special application to calculate major parameters of the motor vehicle and the installed absorber. The article also gives a sensitivity analysis of the effect of the rod length on the decrement of the vehicle's kinetic energy.

1. INTRODUCTION

The importance of passive security in motor vehicles has been growing since decades. The safety of the passenger and the cargo is one of the key issues in transport security. Safety during a car collision with an obstacle is typically ensured by absorbing excessive kinetic energy. To absorb the kinetic energy during a car collision and to convert it into another type of energy, modern motor vehicles use a range of mechanical, hydraulic and pneumatic devices.

Such energy absorbing devices are designed to absorb collision energy and reduce or eliminate its impact on the driver, the passengers or the cargo in the motor vehicle. At the same time, such devices would eliminate the need to use air bags or might be used as an additional means of safety to passengers or the cargo.

The energy absorber is designed as a hydraulic, pneumatic and, at the same time, mechanical device as all these expose specific characteristics that may positively contribute to the overall construction.

The description of the absorber presented here is based on mathematical calculations characterizing mechanical, pneumatic and hydraulic processes in the equipment.

The analysis of the developed mechanism employs a special application to calculate major parameters of the motor vehicle and the installed absorber: the trajectory, velocity, acceleration and kinetic energy of the motor vehicle. The calculations help to determine the significance and variation

of the parameters of individual elements of the absorber. Finally, a research in and an analysis of the sensitivity of the device levers are done.

2. ANALYSIS OF THE CONDUCTED WORK

To absorb motor vehicle's kinetic energy during a collision, various hydraulic, pneumatic or mechanical solutions may be used [10]. Review and analysis of the conducted research distinguishes a hydraulic system [5, 12 - 14], which reduces the impact suffered by the chassis. Also, a pneumatic shock absorbing system [8] and adjustable shock absorbers [9, 16] are widely used to reduce impact on the chassis. The chassis may be equipped with various mechanical [11, 17, 18] or electromechanical safety devices [6, 7] that reduce collision forces when a car with a specially equipped chassis is hit by another motor vehicle.

Mechanical devices [1, 4, 15] may also be used. The development of the construction design has been mostly affected by works by Georg Piontek, Stanislaw Gumula and Premyslaw Lagievka [1-4]. Their works describe a mechanism that changes the force of the forward motion into rotational inertia of a flywheel, along with the other works [12]. The works also present the principle scheme of the mechanism that changes the linear force and kinetic energy of the collision into the flywheel's rotational kinetic energy and torque. They also describe the design of the mechanism, but they present neither calculations of its individual elements nor works of optimization. Another drawback of the presented mechanism is its comparatively large dimensions.

3. A DYNAMIC MODEL OF THE HYDRO PNEUMATIC MECHANICAL ENERGY ABSORBER THAT ENHANCES PASSIVE SAFETY IN MOTOR VEHICLES

A motor vehicle with the mass m_1 has a hydro pneumatic mechanical energy absorber that enhances passive safety in the motor vehicle (Fig. 1). The motor vehicle is coupled with a bumper whose mass is m_2. Between the motor vehicle and the bumper, there is a deformable body with the rigidity of k_{12} and shock absorption c_{12}. As the motor vehicle hits an obstacle with the rigidity of k_0 and shock absorption factor c_0, the part of the device attached to the motor vehicle's bumper begins to move at the velocity v_1. The lever of the device on the left side of the hydraulic cylinder presses the inside liquid, increasing its pressure p_2. The respective piston areas of the hydraulic cylinder on the left and the right sides are A_1 and A_2. The hydraulic cylinder absorbs the initial impact. Perforation in the cylinder partly equalizes the pressure values on both sides of the hydraulic cylinder (p_1 and p_2).

The rack bar attached to the lever lies in the cylinder and moves, on a collision, to the right, rotating the gear wheel mechanism at the same time (the radius of the gear wheel, referred to as the first gear wheel, is marked R_1 in Figs. 1 and 2). During the collision, the gear wheel moving to the right rotates the mechanism and finally (on reaching the end point on the right) comes out of contact with the gear wheel with the radius R_1, leaving the gear wheels and other elements of the mechanism in rotation and movement.

Another gear wheel mounted on axle O_1, or the second gear wheel, with the radius R_2 (Fig. 1 and 2) is coupled with the first gear wheel and rotates at the same speed. The second gear wheel (R_2) is also coupled with the third gear wheel R_3. The gear wheel R_3 is driven by the gear wheel R_2 (Figs. 2 and 3).

The gear wheel R_3 is mounted on axle O_2 with a flywheel (or the fourth gear wheel) with the radius R_4. Also, a traveller L_1 is mounted on the axle O_2 (Fig. 3), which drives a crank L and generates pressure p_4 in the pneumatic cylinder (the piston area is A_4). The pneumatic cylinder absorbs kinetic energy of the flywheel (and the entire mechanism).

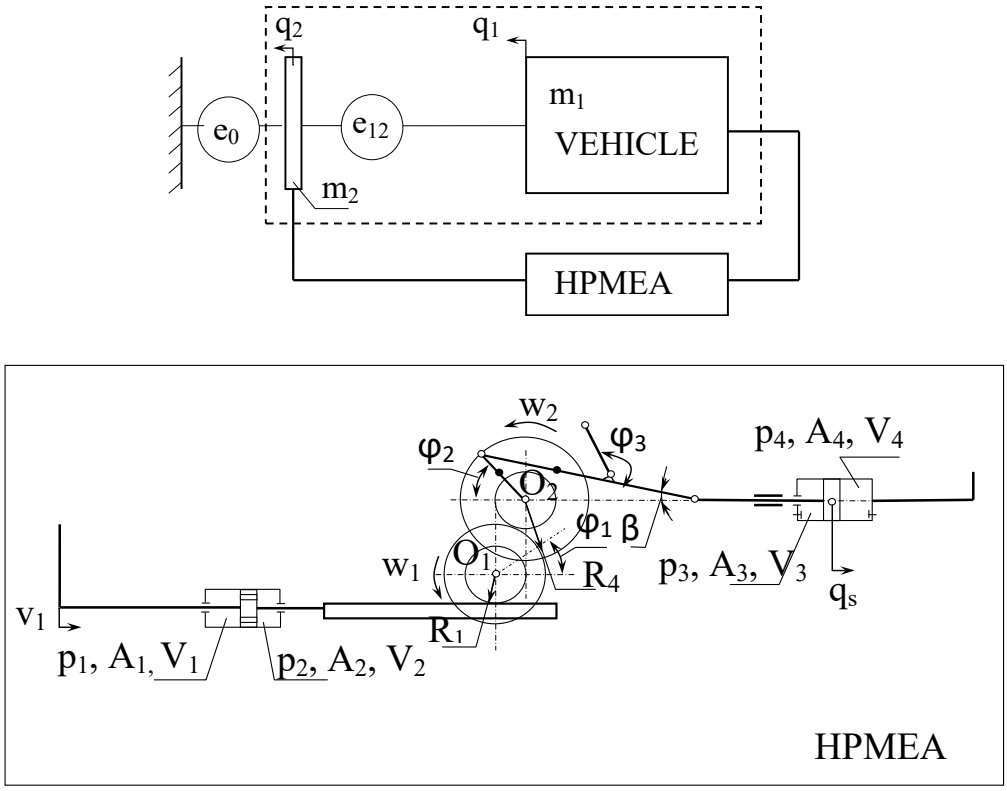

Fig. 1. A dynamic model of the hydro pneumatic mechanical energy absorber that enhances passive safety in motor vehicles

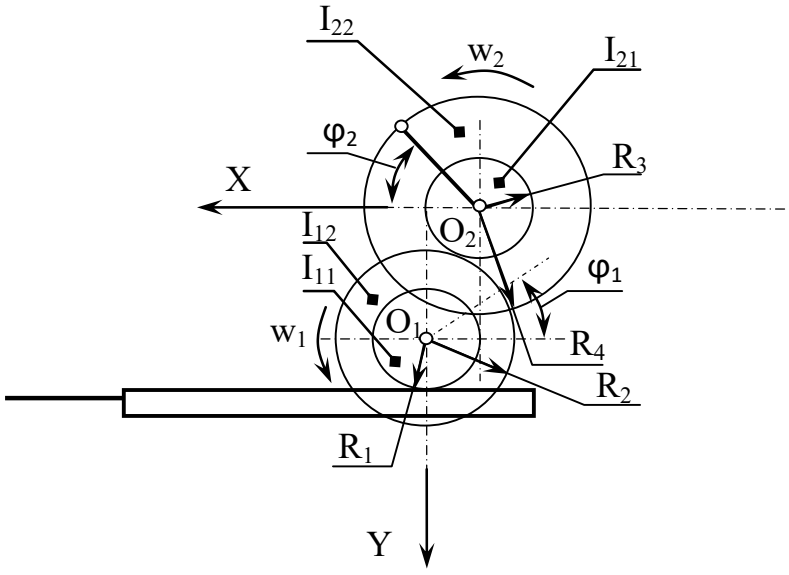

Fig. 2. Assembly of the hydro pneumatic mechanical energy absorber that enhances passive safety in motor vehicles: a rack bar and gear wheels

The centre of gravity of the traveller O_2 is at the distance R_{C2} from the point C_2, and the centre of gravity of the crank C_3 lies at the distance L_2 from the point of connection O_3 (Fig. 3). An additional rod with the length L_4, loaded with an additional mass at its end (point C_4) rotating about the point O_4, is mounted on the crank.

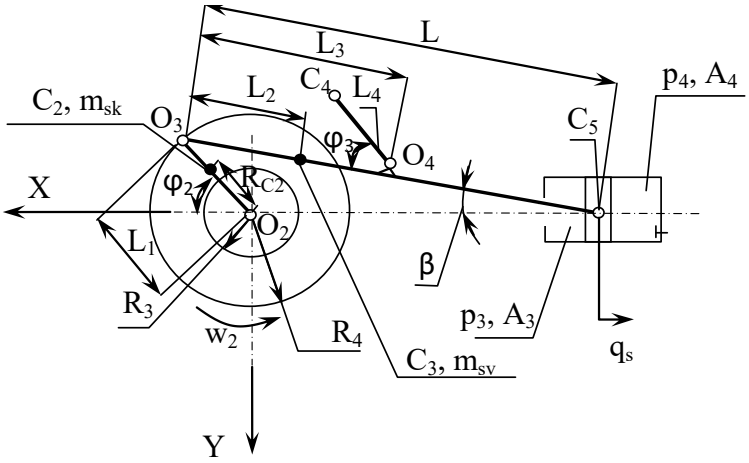

Fig. 3. Assembly of the hydro pneumatic mechanical energy absorber that enhances passive safety in motor vehicles: a flywheel and crank assembly, an additional mass and a pneumatic cylinder

The angular velocity of the gear wheels mounted on axle O_1 is w_1, and the starting position of the first gear wheel is φ_1 (Fig. 1 and 2). The angular velocity of the gear wheels mounted on axle O_2 is w_2 (Fig.1 and 3). The starting point of the traveller is φ_2. The starting point of the additional mass rod C_4 is φ_3 (Fig. 3). The angle of the starting point of the crank measured between the crank L and the axle X is β (Fig. 3). Moments of inertia of the first to fourth gear wheels are given in Fig. 2, with values $I_{11}, I_{12}, I_{21}, I_{22}$, respectively.

The design and parameters of the mechanism have to be set so as to allow the hydro cylinder, the mechanical assembly of the rack bar and the gear wheels, the traveller and the crank with the additional mass on the rod and the pneumatic cylinder to maximally absorb kinetic energy passed to the motor vehicle at the moment of collision with an obstacle. Also, the velocity of the motor vehicle has to maximally decrease, but the acceleration of the motor vehicle should not exceed the value that can cause risk to the driver and the passengers.

4. MATHEMATICAL MODELING OF THE PROCESSES IN THE ENERGY ABSORBER

4.1. Coordinates and velocities of the mechanism

Coordinates and velocities of the actual points in the absorber are described in Fig. 1-3.

Coordinates of the centre of gravity of the traveller are set as follows:

$$x_{c2} = x_{02} + q_1 + R_{c2}\cos\varphi_2 \text{ and} \quad \text{.....(1)}$$

$$y_{c2} = y_{02} - R_{c2}\sin\varphi_2, \quad (2)$$

where x_{02} and y_{02} are coordinates X and Y of the traveller's centre of rotation about the point O_2; q_1 is the vehicle's displacement; R_{c2} is the distance from the centre of rotation O_2 to the centre of gravity C_2; and φ_2 is the turning angle of the traveller X in respect of its axle.

Velocity of the centre of gravity of the traveller is X and Y in respect of X and Y coordinates:

$$\dot{x}_{c2} = \dot{q}_1 - R_{c2}\dot{\varphi}_2\sin\varphi_2 \text{ and} \quad (3)$$

$$\dot{y}_{c2} = -R_{c2}\dot{\varphi}_2\cos\varphi_2, \quad (4)$$

where $\dot{q}_1$ is the velocity of the motor vehicle and $\dot{\varphi}_2$ is the angular velocity of the traveller.

The coordinates of the traveller's end point O_3 are determined as follows:

$$x_{O3} = x_{O2} + q_1 + L_1\cos\varphi_2 \text{ and} \quad (5)$$

$$y_{O3} = y_{O2} - L_1\sin\varphi_2, \quad (6)$$

and their velocities are as follows:

$$\dot{x}_{O3} = \dot{q}_1 - L_1\dot{\varphi}_2 \sin\varphi_2 \text{ and} \tag{7}$$

$$\dot{y}_{O3} = -L_1\dot{\varphi}_2 \cos\varphi_2, \tag{8}$$

where L_1 is the length of the traveller.

The coordinates of the centre of gravity of the crank C_3 are as follows:

$$x_{c3} = x_{O3} - L_2 \cos\beta \text{ and} \tag{9}$$

$$y_{c3} = y_{O3} + L_2 \sin\beta, \tag{10}$$

and their velocities are as follows:

$$\dot{x}_{c3} = \dot{q}_1 - L_1\dot{\varphi}_2 \sin\varphi_2 + L_2\dot{\beta}\sin\beta \text{ and} \tag{11}$$

$$\dot{y}_{c3} = -L_1\dot{\varphi}_2 \cos\varphi_2 + L_2\dot{\beta}\cos\beta, \tag{12}$$

where L_2 is the distance from the point of connection of the traveller with the crank and the centre of gravity of the crank C_3; β is the angle between the crank and axis X; and $\dot{\beta}$ the angular velocity of the crank in respect of axis X.

Coordinates of the point O_4 of the rod attached to the crank at the point O_4 are as follows:

$$x_{O4} = x_{O3} - \cos\beta \text{ and} \tag{13}$$

$$y_{O4} = y_{O3} + L_3 \sin\beta, \tag{14}$$

and their velocities are as follows:

$$\dot{x}_{O4} = \dot{q}_1 - L_1\dot{\varphi}_2 \sin\varphi_2 + L_3\dot{\beta}\sin\beta \text{ and} \tag{15}$$

$$\dot{y}_{O4} = -L_1\dot{\varphi}_2 \cos\varphi_2 + L_3\dot{\beta}\cos\beta, \tag{16}$$

where L_3 is the distance between the point of connection of the traveller to the crank O_3 and the point of the rod attachment to the crank O_4.

Coordinates of the rod connection point O_4 and the rotating end point C_4 are determined as follows:

$$x_{c4} = x_{O4} + L_4 \cos(\beta + \varphi_3) \text{ and} \tag{17}$$

$$y_{c4} = y_{O4} - L_4 \sin(\beta + \varphi_3), \tag{18}$$

where L_4 is the length of the rod O_4C_4 and φ_3 is the turning angle between the rod O_4C_4 and the crank.

The elocity of the rotating end point C_4 of the rod attached at the point O_4 is determined as follows:

$$\dot{x}_{c4} = \dot{q}_1 - L_1\dot{\phi}_2 \sin\phi_2 + L_3\dot{\beta}\sin\beta - L_4(\dot{\beta} + \dot{\phi}_3)\sin(\beta + \phi_3), \tag{19}$$

$$\dot{y}_{c4} = -L_1\dot{\phi}_2 \cos\phi_2 + L_3\dot{\beta}\cos\beta - L_4(\dot{\beta} + \phi_3)\cos(\beta + \phi_3), \tag{20}$$

where $\dot{\varphi}_3$ is the angular velocity of the rod O_4C_4.

Coordinates of the end point of the traveller C_5, which coincide with coordinates of the piston of the pneumatic cylinder, are following:

$$x_{c5} = x_{O3} - L\cos\beta \text{ and} \tag{21}$$

$$y_{c5} = y_{O3} + L\sin\beta, \tag{22}$$

and the velocity of the point C_5 is as follows:

$$\dot{x}_{c5} = \dot{q}_1 - L_1\dot{\varphi}_2 \sin\varphi_2 + L\dot{\beta}\sin\beta, \tag{23}$$

where L is the length of the crank.

4.2. Kinetic and potential energy of the absorber

The kinetic energy of the system is equal to the following:

$$E_k = \frac{1}{2}m_1\dot{q}_1^2 + \frac{1}{2}m_2\dot{q}_2^2 + \frac{1}{2}I_{12}\dot{\phi}_1^2 + \frac{1}{2}I_{21}\dot{\phi}_2^2 + \frac{1}{2}I_{22}\dot{\phi}_2^2 + \frac{1}{2}m_{c2}(\dot{x}_{c2}^2 + \dot{y}_{c2}^2) + \\ + \frac{1}{2}m_{c3}(\dot{x}_{c3}^2 + \dot{y}_{c3}^2) + \frac{1}{2}m_{c4}(\dot{x}_{c4}^2 + \dot{y}_{c4}^2) + \frac{1}{2}m_{c5}\dot{x}_{c5}^2, \tag{24}$$

where m_1 and m_2 are the respective masses of the motor vehicle and the bumper; $\dot{q}_1$ and $\dot{q}_2$ are the respective accelerations of the motor vehicle and the bumper; I_{12}, I_{21}, I_{22} are the moments of inertia of the gearwheels, whose radii are R_2, R_3 and R_4, respectively; m_{c2} is the mass of the traveller; m_{c3} is the mass of the crank; m_{c4} is the mass of the rod attached to the crank at the point C_4; and m_{c5} is the velocity of the piston of the pneumatic cylinder.

The potential energy of the system is equal to the following:

$$E_p = \frac{1}{2}k_{12}(q_2 - q_1)^2 + \frac{1}{2}k_0 q_2^2 H(q_2 - \Delta_0) + \frac{1}{2}k_{23}(-q_2 - R_1\phi_1)^2 + \frac{1}{2}k_{34}(R_1\phi_1 - R_2\phi_2)^2, \tag{25}$$

where k_0 is the obstacle's rigidity factor; k_{12} is the rigidity factor of the motor vehicle and the bumper assembly; k_{23} is the rigidity factor between the rack bar and the first gear wheel (with the radius R_1); k_{34} is the rigidity factor between the second and the third gear wheels; the respective radii are R_2 and R_3; H is the Heaviside function; Δ_0 is the initial distance between the bumper of the motor vehicle and the obstacle; and R_1 and R_2 are the radii of the first and the second gear wheels (the axis of rotation is O_1).

4.3. Generalized forces

Generalized forces of the assembly are the following:

$$m_2\ddot{q}_2 = -p_1A_1 + p_2A_1 - F_{tr12}sign(\dot{q}_2 - \dot{q}_1); \tag{26}$$

$$m_1\ddot{q}_1 = Q_1 - F_{tr12}sign(\dot{q}_1 - \dot{q}_2) - F_{trcil}sign\dot{q}_s, \tag{27}$$

where m_1 and m_2 are the respective masses of the motor vehicle and the bumper; $\ddot{q}_1$ and $\ddot{q}_2$ are the respective accelerations of the motor vehicle and the bumper; p_1 and p_2 are the pressure values in the left and the right chamber of the cylinder, respectively; A_1 is the piston area in the left side of the cylinder; F_{tr12} is the friction force between the motor vehicle and the bumper; $\dot{q}_1$ and $\dot{q}_2$ are the respective accelerations of the motor vehicle and the bumper; F_{trcil} is the friction between the hydraulic cylinder and the piston; and $\dot{q}_s$ is the velocity of the piston.

4.4. Equation for pressure change in the hydraulic and the pneumatic cylinders

The force of the piston in the hydraulic cylinder is described as follows:

$$F_s = A_4p_4 - A_3p_3 \tag{28}$$

where A_3 and A_4 are piston areas on the left and the right sides of the pneumatic cylinder and p_3 and p_4 are pressure values on the left and the right sides of the piston in the pneumatic cylinder.

The pressure change in the first chamber of the hydraulic cylinder is described by the following equation:

$$\dot{p}_1 = \frac{K}{v_{10} + A_1(q_1 - q_2)}\left[Q_{12}sign(p_2 - p_1) - A_1(\dot{q}_1 - \dot{q}_2)\right], \tag{29}$$

where K is the volumetric modulus of elasticity of the fluid; V_{10} is the initial volume of the first chamber; A_1 is the piston area in the left side of the hydraulic cylinder; Q_{12} is the fluid debit between the first and the second chamber of the hydraulic cylinder; and p_1 and p_2 are the pressure values in the left and the right sides of the cylinder, respectively.

Pressure change in the second (right) chamber of the hydraulic cylinder is described by the following equation:

$$\dot{p}_2 = \frac{K}{v_{20} + A_2(q_2 - q_1)}\left[-Q_{12}sign(p_2 - p_1) - A_2(\dot{q}_2 - \dot{q}_1)\right], \tag{30}$$

where V_{20} is the initial volume of the second chamber and A_2 is the piston area in the right side of the hydraulic cylinder.

$$Q_{12} = \frac{A_{12}}{\sqrt{\varepsilon_{12}(\mathrm{Re})}}\sqrt{\frac{2}{\rho}|p_2 - p_1|}, \tag{31}$$

where A_{12} is the perforation area of the piston of the hydraulic cylinder; ε_{12} is the fluent deficiency rate in the perforation of the piston; Re is the Reynolds number; and ρ is the density of the fluid.

Pressure change in the left chamber of the hydraulic cylinder is described by the following equation:

$$\dot{p}_3 = \frac{\gamma RT}{v_{30} + A_3 q_{st}}(G_3(p_\infty - p_3)) - (\frac{\gamma p_3}{v_{30} + A_3 q_{st}}(A_3\dot{q}_{st})), \tag{32}$$

where γ is the gas adiabatic index; R is the gas constant; T is the temperature; V_{30} is the initial volume of the third chamber of the pneumatic cylinder; A_3 is the piston area in the left side of the pneumatic cylinder; q_{st} is the displacement of the piston of the pneumatic cylinder; G_3 is the rate of the gas flow from the third chamber to the environment; p_∞ is the ambient pressure; and p_3 is the pressure value on the left side of the pneumatic cylinder.

On the right side of the pneumatic cylinder: Pressure change in the right chamber of the hydraulic cylinder is described by the following equation:

$$\dot{p}_4 = \frac{\gamma RT}{v_{40} - A_4 q_{st}}(-G_{34}sign(p_4 - p_3)) - \frac{\gamma p_4}{v_{40} - A_4 q_{st}}(-A\dot{q}_{st}), \tag{33}$$

where V_{40} is the initial volume of the fourth chamber; A_4 is the piston area in the right side of the pneumatic cylinder; G_{34} is the rate of the gas flow between the third and the fourth chamber; and p_4 is the pressure value on the right side of the pneumatic cylinder.

Piston displacement in the hydraulic cylinder is as follows:

$$q_{st} = x_{02} + q_1 + L_1\cos\varphi_2 - L\cos\beta, \tag{34}$$

where x_{02} is the initial coordinate of the piston; L and L_1 are the respective lengths of the crank and the traveller; φ_2 is the angle between the traveller and its axle X; and β is the angle between the crank and its axle X.

4.5. Equations to describe the movement of the gear wheels in the assembly

The movement of the gear wheels is described by the following equations:

$$(I_{11} + I_{12})\ddot{\varphi}_1 = -k_{23}R_1(q_2 - \Delta_0 + R_1\varphi_1)H(-\Delta_0 + q_2 + R_1\varphi_1) - c_{23}R_1(\dot{q}_2 + R_1\dot{\varphi}_1)H(-\Delta_0 + q_2 + R_1\varphi_1) + c_{34}R_2(-R_2\dot{\varphi}_1 - R_3\dot{\varphi}_2)H(-R_2\varphi_1 - R_3)\varphi_2 + \Delta_{340}). \tag{35}$$

$$(I_{21} + I_{22})\ddot{\phi}_2 = R_3k_{34}(-R_2\phi_1 - R_3\phi_2 + \Delta_{320})H(-R_3\phi_1 - R_3\phi_3 + \Delta_{340}) + R_3c_{34}(-R_2\ddot{\phi}_1 - R_3\dot{\phi}_2)H(-R_3\phi_1 - R_3\phi_2 + \Delta_{340}), \tag{36}$$

where I_{11}, I_{12}, I_{21}, and I_{22} are the respective moments of inertia of the gear wheels; $\ddot{\varphi}_1$ and $\ddot{\varphi}_2$ are the acceleration values; R_1, R_2, and R_3 are the radii of the respective gear wheels; k_{23} and k_{34} are the gear wheels coupling rigidity factors; Δ_0 is the distance between the bumper and the obstacle; Δ_{320} and Δ_{340} are the initial gaps between the gear wheel teeth in the coupling; H is the Heaviside function; and c_{23} and c_{34} are the decrement indexes.

5. DEVELOPMENT OF THE APPLICATION

To carry out the exact calculations of the parameters of the hydro pneumatic mechanical energy absorber, based on the formulas described in chapter 4, a special FORTRAN application has been developed.

The calculations include the following parameters:

- ✓ masses of the motor vehicle, the bumper, the crank, the traveller, the pneumatic piston and the gear wheels;
- ✓ radii of the gear wheels;
- ✓ moments of inertia of the gear wheels;
- ✓ distances from the points of connection of the traveller, the crank and the additional mass to the corresponding centres of gravity;
- ✓ diameters of the pistons and the rods;
- ✓ the number and diameters of the holes in the hydraulic piston;
- ✓ clearance between the rack bar and the gear wheel, and clearance between gear wheels (the second and the third gear wheels);
- ✓ the volumetric modulus of elasticity and density of the fluid.

6. RESULTS OF MATHEMATICAL CALCULATIONS

For the actual calculations, the following parameters have been chosen: 1000 kg vehicle mass, 20 kg bumper mass and 40 km/h motor vehicle's velocity. The calculations include the following parameters of the hydraulic and pneumatic cylinders: moments of inertia and radii of the gear wheels, weights and lengths of the traveller and the crank. The major parameters are presented in the table below.

Further analysis of the device parameters comprises vehicle and bumper thrust, velocities, and accelerations, turning angles of the gearwheels and the traveller, piston strokes and velocities, and the mechanism inertia. The most important among them are thrust, velocity, acceleration and kinetic energy of the vehicle.

The obtained results are graphically presented in Figs. 4–7.

The analysed device is designed to absorb vehicle collision energy; therefore, the optimal parameters have to be set so as to suppress maximum kinetic energy of the vehicle in the shortest possible time on its collision with an obstacle. Meanwhile, the motor vehicle's displacement should remain minimum and its acceleration value should remain within the allowable range.

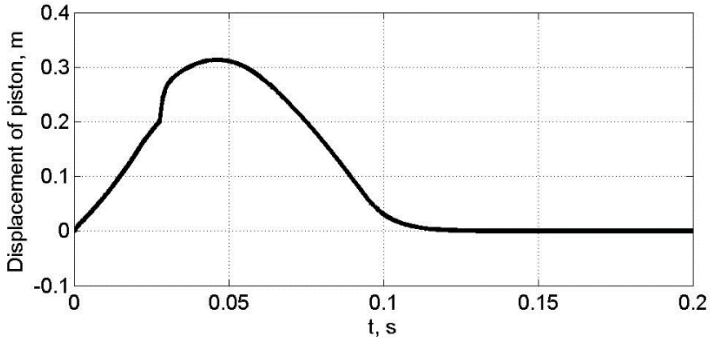

Fig. 4. Displacement (m) of piston when the vehicle with the energy absorber hits an obstacle at the speed of 40 km/h

7. SENSITIVITY ANALYSIS OF THE PARAMETERS OF THE HYDRO PNEUMATIC MECHANICAL ENERGY ABSORBER

To correctly select parameters of the assembly, it is necessary to know which of them have the most significant effect on the reduction of the system's kinetic energy. The actual effect of each parameter on the reduction of the system's kinetic energy is determined as follows:

$$s_k = \frac{\partial E_k}{\partial par_k} / \frac{E_{k,\max}}{par_{0,k}}, \tag{37}$$

where $E_{k,\max}$ and E_k are the respective kinetic energy values of the motor vehicle and the bumper and $par_{0,k}$ is the nominal value of parameter k.

Table 1

Major parameters of the device

Selected parameter	Parameter value
Rack bar to gear wheel engagement throw, mm	100
Traveller length, L_1, mm	150
Traveller L_1 weight, kg	2
Crank length L, mm	400
Crank L weight, kg	3
Additional mass rod L_3 length, mm	100
Additional mass at point C_4, kg	5
Radius of the first gear wheel R_1 , mm	70
Radius of the second gear wheel R_2 , mm	100
Radius of the third gear wheel R_3 , mm	70
Radius of the fourth gear wheel R_4 , mm	150
Weight of the first gear wheel R_1 , kg	2
Weight of the second gear wheel R_2 , kg	4
Weight of the third gear wheel R_3 , kg	2
Weight of the fourth gear wheel R_4 , kg	5
Number and diameter of the holes in the hydraulic piston, units × mm	4×5
Diameter of the hydraulic piston, mm	150
Diameter of the hydraulic piston rod, mm	10
Bulk modulus of elasticity, GPa	1,0

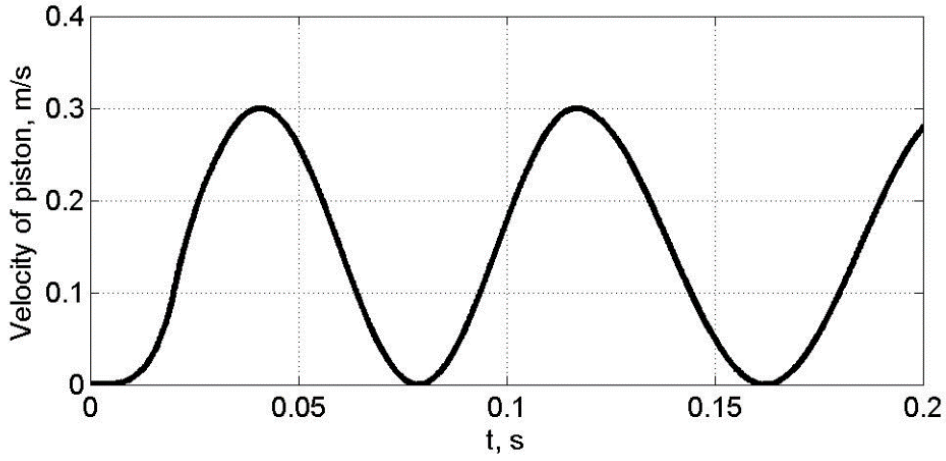

Fig. 5. Velocity (m/s) of piston when the vehicle with the energy absorbing device hits an obstacle at the speed of 40 km/h

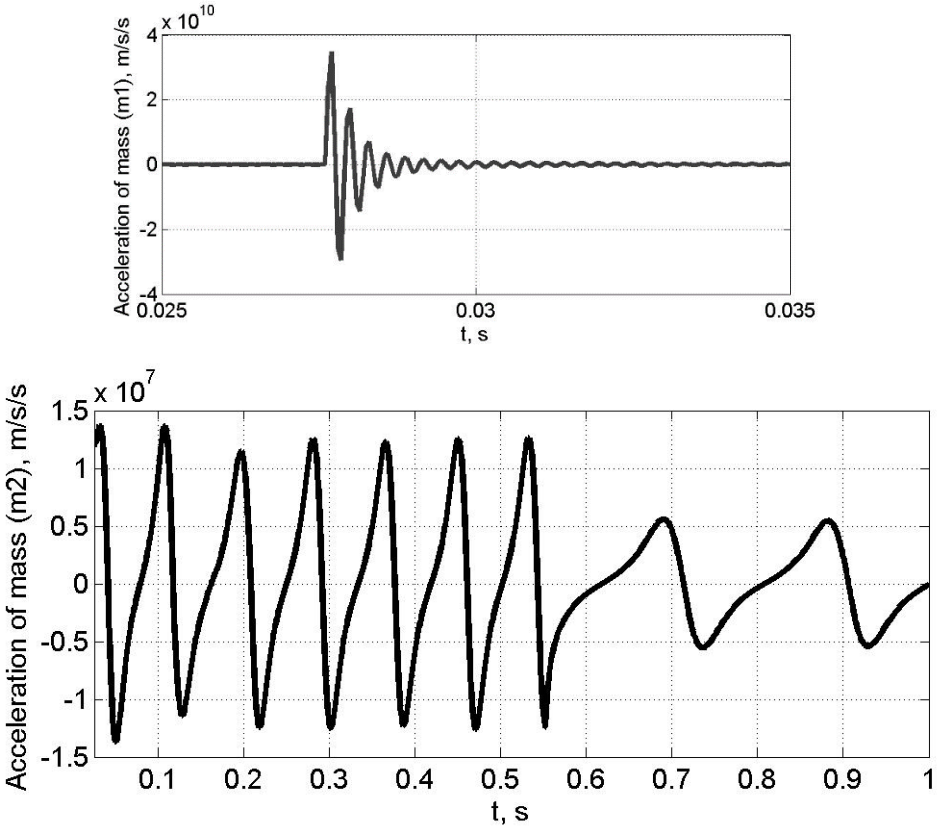

Fig. 6. Acceleration of mass when the initial velocity is 40 km/h

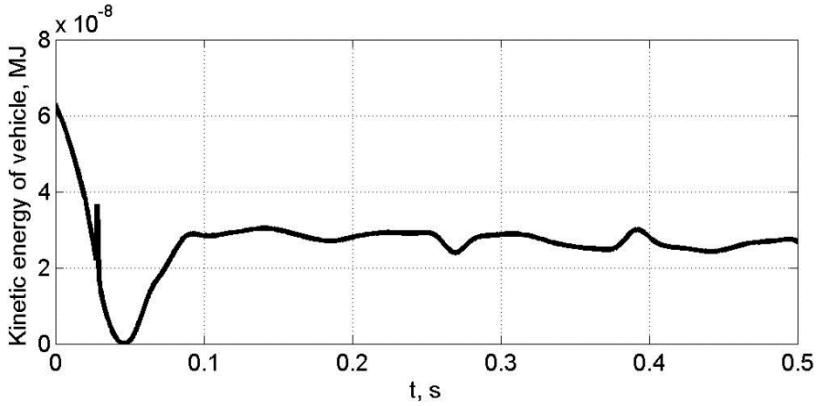

Fig. 7. Kinetic energy of vehicle shifts when the initial velocity is 40 km/h

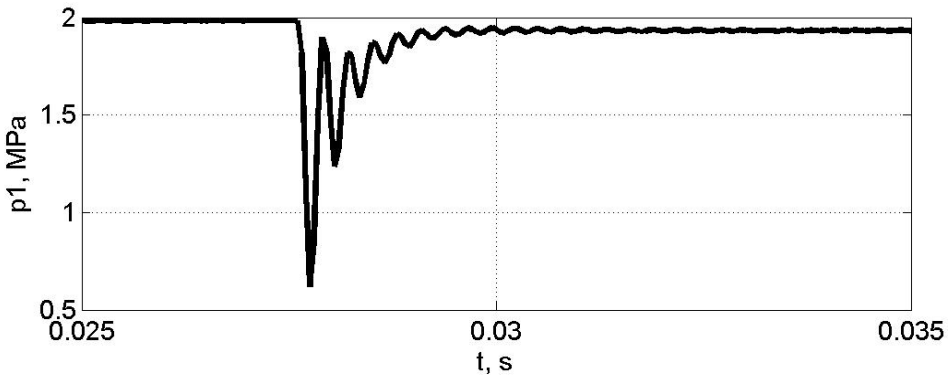

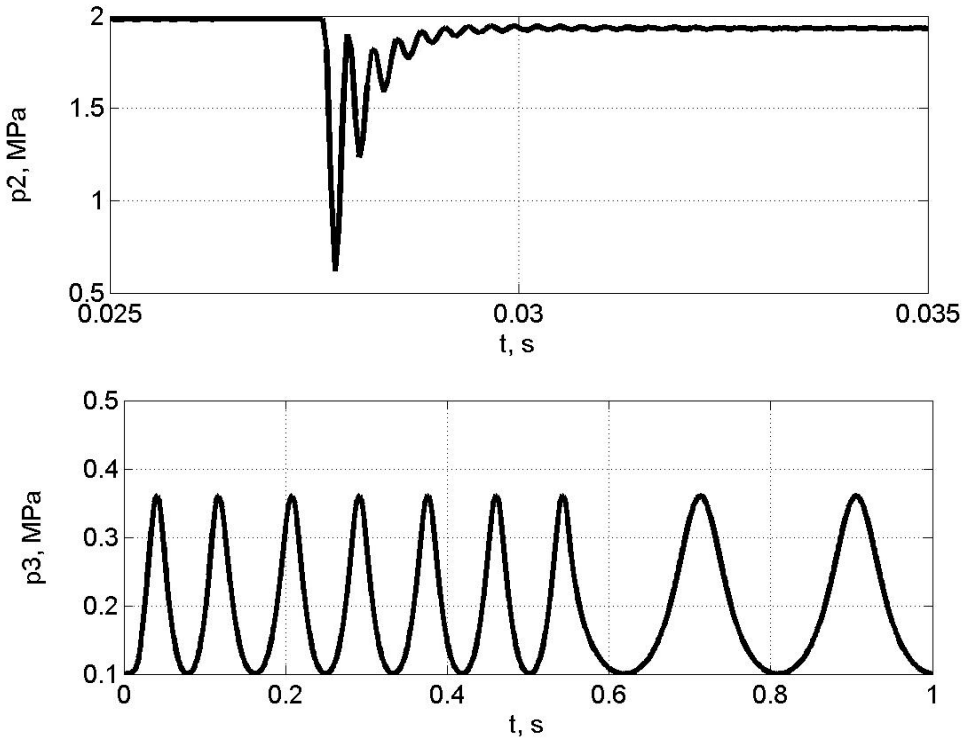

Fig. 8. Pressure of hydraulic cylinder volumes when the initial velocity is 40 km/h

The present research aims to find out the system's parameters that have the most significant effect on reduction of the system's kinetic energy at different initial velocities of the motor vehicle.

First, the actual lengths of the moving parts have been selected (see Fig. 3). The impact of the length of the moving parts of the device on the reduction of the system's kinetic energy has been analysed at the initial speed values (prior to the collision) of 26, 50, 70, 90, 110 and 130 km/h: 26 km/h as an average motor vehicle's speed in urban locations; 50 km/h as a speed limit in urban locations; 70 km/h as a speed limit on high speed streets; 90 km/h as a speed limit on rural roads; 110 km/h as a speed limit on motorways in winter; and 130km/h as a maximum allowable speed on motorways.

Table 2

Absorber's moving parts ranking table (the parts are ranked in accordance to the impact of their length on reduction of the system's kinetic energy)

No.	Part lettering (Fig. 3)	Velocity before engagement with an obstacle						Total	Significance
		26	50	70	90	110	130		
1	L	3	4	3	3	3	4	20	3
2	L_1	1	1	1	1	1	1	6	1
3	L_2	5	5	5	5	5	5	30	5
4	L_3	4	3	4	4	4	3	22	4
5	L_4	2	2	2	2	2	2	8	2

To find out the most influencing moving part of the mechanism at various velocities, a ranking table (Table 2) has been compiled. Here, the part with the most significant impact on the assembly's kinetic energy is marked 1, the second most significant part is marked 2 and so on.

The conducted summary analysis reveals that the systems' kinetic energy is mostly affected by the length of the traveller L_1, then subsequently, the length of the additional rod L_4 (fixed at the point O_4), the length of the crank L, the distance L_3 between the point of connection of the traveller to the crank O_3 and the point O_4, and the distance between the point of connection of the traveller to the crank O_3 and the centre of gravity of the crank L_2.

8. CONCLUSIONS

1. The present work has proposed a hydro pneumatic mechanical device designed to inhibit motor vehicle's energy on a collision with an obstacle.
2. On the first contact with the obstacle, the peak load is sustained by the hydraulic cylinder wherein the vehicle's kinetic energy is transformed into potential energy of the hydraulic fluid in the cylinder.
3. During the subsequent stages of the collision, the vehicle's kinetic energy is transformed into kinetic energy of the mechanical part of the device and potential energy of the pneumatic cylinder.
4. The hydro pneumatic mechanical energy absorber absorbs more than 50 percent of the car's kinetic energy in 0.1 s, if the car's speed is 40 km/h. Other parameters of the hydro pneumatic mechanical energy absorber are shown in the table.
5. The analysis of the impact of the lengths of the moving parts of the energy absorber on the reduction of the system's kinetic energy has revealed that the reduction of the system's kinetic energy is mostly dependent on (in descending order) the following: the length of the traveller L_1, the length of the additional rod L_4 and the length of the crank L (Fig. 3).
6. To increase absorption of energy by the system, lengths of the traveller L_1 and the additional rod L_4 have to be enlarged.
7. Further, a test speed interval should be set for the motor vehicle, and efficiency of the absorber should be analysed (on the basis of diagrams of the dissipative function indicating energy absorption capacity) at various speed values.

References

1. Gumuła, S. & Doruch, H. Układy do hamowania i zabezpieczania pojazdów przed skutkami zderzeń poprzez przekazanie energii akumulatorom mechanicznym. *Proceedings of the VI Sympozjum Naukowo-Techniczne - SILWOJ' 2003.* 2003. P. 209-214. [In Polish: Systems for braking and protecting vehicles against the effects of collisions by transferring energy to mechanical batteries].
2. Gumuła, S. & Łągiewka, L. A method of impact and inertia force reduction during collisions between physical objects. Results of experimental investigations. *Journal of Technical Physics.* 2007. No. 48(1). P. 13-27.
3. Gumuła, S. & Łągiewka, L. Conceptual design of vehicles' protection against the impacts of collisions using the energy transfer method. *Journal of KONES Powertrain and Transport.* 2006. No. 13(1). P. 269-277.
4. Gumuła, S. & Łągiewka, L. Zmniejszanie siły zderzeń. *Przegląd Techniczny*. 2005. No. 2. [In Polish: Reducing collision strength. *Technical review*].
5. US 2010/0122864 A1. Hybrid hydraulic drive system for all terrestrial vehicles, with the hydraulic accumulators as the vehicle chassis. Available at: http://www.google.com/patent/US2010012286.

6. WO 2013137516 A1. A Vehicle bumper where the shock absorber which uses permanent magnet and electromagnet is established.
Available at: http://www.google.com/patents/WO2013137516A1?cn.
7. CN 201833977. Vehicle safety mechanism. Available at: http://www.google.com/patents/ CN201833977U?cl=zh.
8. CN 201989737. Special vehicle chassis gas circuit control device.
Available at: http://www.google.com/patents/CN201989737U?cl=zh.
9. DE 10 2010 051 872 A1. Die folgenden Angaben sind den vom Anmelder eingereichten entnommen [online]. Available at: http://www.google.com/patents/ DE102011104016B4?cl=en.
10. Huang, X. & Xie, Y.M. & Lu, G. Topology optimization of energy- absorbing structures. *International Journal of Crashworthiness*. 2007. 12:6. P. 663-675. DOI: 10.1080/13588260701497862.
11. Simon, P. & Beggs, P.D. A numerical performance comparison of a dual-phase steel and aluminium alloy bumper bar system. *International Journal of Crashworthiness*. 2010. Vol. 15(4). P. 425-442. DOI: 10.1080/13588261003696441.
12. Cronk, P.M. & Van de Ven, J.D. A review of hydro-pneumatic and flywheel energy storage for hydraulic systems. *International Journal of Fluid Power*. 2018. Vol. 19(2). P. 69-79. DOI: 10.1080/14399776.2017.1386061.
13. Caihong Huang & Jing Zeng. Dynamic behaviour of a high- speed train hydraulic yaw damper. *Vehicle System Dynamics.* 2018. Vol. 56(12). P. 1922-1944. DOI: 10.1080/00423114.2018.1439588.
14. Van de Ven, J.D. Increasing Hydraulic Energy Storage Capacity: Flywheel-Accumulator. *International Journal of Fluid Power*. 2009. Vol. 10(3). P. 41-50. DOI: 0.1080/14399776.2009.10780987.
15. Kokkula, S. & Langseth, M. & Hopperstad, O.S. & Lademo, O-G. Offset impact behaviour of bumper beam—longitudinal systems: experimental investigations. *International Journal of Crashworthiness.* 2006. Vol. 11(4). P. 299-316. DOI: 10.1533/ijcr.2005.012.
16. Sijing Guo, & Yilun Liu & Lin Xu & Xuexun Guo & Lei Zuo. Performance evaluation and parameter sensitivity of energy-harvesting shock absorbers on different vehicles. *Vehicle System Dynamics.* 2016. Vol. 54(7). P. 918-942. DOI: 10.1080/00423114.2016.1174276.
17. Ruiming Zou, Shihui Luo & Weihua Ma. Simulation analysis on the coupler behaviour and its influence on the braking safety of locomotive. *Vehicle System Dynamics*. 2018. Vol. 56(11). P. 1747-1767. DOI: 10.1080/00423114.2018.1435893.
18. Griškevičius, P. & Žiliukas, A. The crash energy absorption of the vehicles front structures. *Transport.* 2003. Vol. 18(2). P. 97-101.

Received 13.02.2018; accepted in revised form 31.05.2019